

RSC Advances



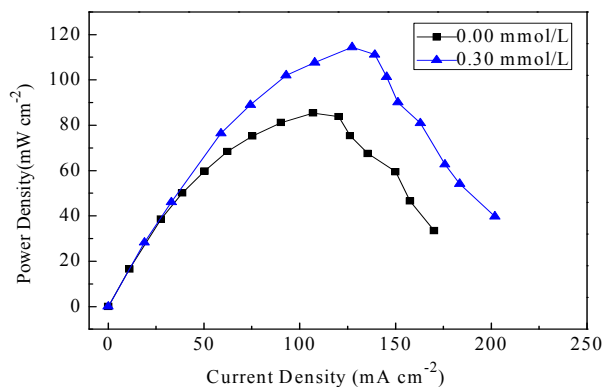
This is an *Accepted Manuscript*, which has been through the Royal Society of Chemistry peer review process and has been accepted for publication.

Accepted Manuscripts are published online shortly after acceptance, before technical editing, formatting and proof reading. Using this free service, authors can make their results available to the community, in citable form, before we publish the edited article. This *Accepted Manuscript* will be replaced by the edited, formatted and paginated article as soon as this is available.

You can find more information about *Accepted Manuscripts* in the [Information for Authors](#).

Please note that technical editing may introduce minor changes to the text and/or graphics, which may alter content. The journal's standard [Terms & Conditions](#) and the [Ethical guidelines](#) still apply. In no event shall the Royal Society of Chemistry be held responsible for any errors or omissions in this *Accepted Manuscript* or any consequences arising from the use of any information it contains.

The effect of sodium stannate as the electrolyte additive on the electrochemical performances of the Mg-8Li-1Y electrode in NaCl solution



Mg-8Li-1Y electrode as the anode of Mg-H₂O₂ semi-fuel cells with 0.30 mmol/L Na₂SnO₃ additive displays better performances than without Na₂SnO₃.

The effect of sodium stannate as the electrolyte additive on the electrochemical performances of the Mg-8Li-1Y electrode in NaCl solution

*Yan-Zhuo Lv,¹ * Yan-Zhang Jin,¹ Zhen-Bo Wang,² Yan-Feng Li,¹ Li Wang,¹ Dian-Xue Cao¹*

¹ College of Material Science and Chemical Engineering, Harbin Engineering University, Harbin, 150001 China, ² School of Chemical Engineering and Technology, Harbin Institute of Technology, No. 92 West-Da Zhi Street, Harbin, 150001 China,

*To whom all the correspondence should be addressed. E-mail: lvyanzhuo@hrbeu.edu.cn

Abstract

The effect of different concentrations of sodium stannate (Na_2SnO_3) as the electrolyte additive in 0.7 mol L^{-1} NaCl electrolyte solution on the electrochemical performances of the Mg-8Li-1Y alloy electrode prepared by the vacuum induction melting method have been investigated by means of potentiostatic current-time, potentiodynamic polarization, electrochemical impedance spectroscopy measurements and scanning electron microscopy examination. The performances of the magnesium-hydrogen peroxide ($\text{Mg-H}_2\text{O}_2$) semi-fuel cells with the Mg-8Li-1Y alloy as the anode were also determined. From the study, it has been found that the corrosion potential of the Mg-8Li-1Y electrode is slightly shifted to the negative direction and the corrosion current density is markedly decreased when the different

concentrations of Na_2SnO_3 are added into 0.7 mol L^{-1} NaCl electrolyte solution. The electrochemical impedance spectroscopy measurements show that the polarization resistance of the Mg-8Li-1Y electrode reduces in the following order with the concentrations of Na_2SnO_3 : $0.20 \text{ mmol L}^{-1} > 0.00 \text{ mmol L}^{-1} > 0.05 \text{ mmol L}^{-1} > 0.10 \text{ mmol L}^{-1} > 0.30 \text{ mmol L}^{-1}$. The potentiostatic current-time curves of the Mg-8Li-1Y electrode in 0.7 mol L^{-1} NaCl electrolyte solution containing 0.30 mmol L^{-1} Na_2SnO_3 have revealed better electrochemical performances than that in the other concentrations. The addition of Na_2SnO_3 to the NaCl electrolyte solution loosens the product film and changes the size and thickness of the micro-clumps of the oxidation products. The Mg- H_2O_2 semi-fuel cell with the Mg-8Li-1Y anode in 0.7 mol L^{-1} NaCl solution containing 0.30 mmol L^{-1} Na_2SnO_3 presents a maximum power density of 112 mW cm^{-2} at room temperature.

1. Introduction

The Mg- H_2O_2 semi-fuel cell has received considerable attention in recent years, because it has many advantages, such as low cost, high power density, stable discharging current density, high specific energy, ability to work at ambient pressure, environmental friendliness, reliability, safety and so on¹⁻⁸. These properties make Mg- H_2O_2 semi-fuel cells the promising candidates in a wide range of fields containing space flight and automobile around the world. In addition, it also can be used in carry-home light equipment, automobile, medical and physical appliances for the convenience of movement.

This electrochemical system consists of a magnesium alloy anode, sodium chloride anolyte, cathode catalyst, conductive membrane and catholyte of sodium

chloride, sulfuric acid and hydrogen peroxide. Magnesium is an attractive anode material for this type of semi fuel cell, because magnesium has high Faradaic capacity (Mg: 2.2 Ah g^{-1}), high specific energy (Mg: 6.8 kW h kg^{-1}), more negative standard electroreduction potential versus standard hydrogen electrode (Mg: -2.37 V in neutral solution)⁹. Mg-H₂O₂ semi-fuel cell has a theoretical voltage of 4.14 V , which is higher than that of Al-H₂O₂ semi-fuel cell^{10, 11} and Al-AgO battery. Magnesium alloys as the anodes have been widely investigated since the 1960s, such as AZ31 and AZ61.

However, in practical, these electrodes operate at significantly less negative potentials, resulting from the fact that magnesium anodes are normally covered by passive oxide films which cause a delay in reaching a steady-state and reduce discharging rate. In addition, the parasitic corrosion reactions or self discharge result in the reduction of columbic efficiency of Mg alloys¹². In general, there are two ways to improve the anode performance. Firstly, magnesium is doped with other elements, such as lithium, aluminum, cerium, yttrium¹³. Lv et al. investigated that the effect of the alloy elements (Al, Zn, Y) on the electrochemical performances of the Mg-8Li alloys in 0.7 mol L^{-1} NaCl electrolyte solution^{14, 15}. Secondly, the additives are added into the electrolyte to activate the anode or to prevent the formation of the oxidation products on the anode. For instance, in our previous study, Cao added oxides of gallium into the solution system, and then further improvement of discharge current densities of Mg-Li alloys were obtained due to the addition of additives¹². Indeed, similar results were found by some other researchers that zinc, calcium and indium as

well as stannates (aluminium/air batteries) and citrates were discovered to be the effective electrolyte additives for inhibiting corrosion and/or boosting the electrode potential¹⁶⁻¹⁹.

In this study, the Mg-8Li-1Y alloy was fabricated and its electrochemical performances were evaluated in 0.7 mol L⁻¹ NaCl electrolyte solution containing different concentrations of Na₂SnO₃. The influence of the concentrations of Na₂SnO₃ in 0.7 mol L⁻¹ NaCl solution on the electrochemical behaviors of the Mg-8Li-1Y electrode was investigated. The performances of Mg-H₂O₂ semi-fuel cells with the Mg-8Li-1Y anodes were also evaluated.

2. Experimental

2.1. Preparation of the Mg-8Li-1Y alloys

The Mg-8Li-1Y alloys were prepared from ingots of pure magnesium (99.99%), pure lithium (99.99%), Mg-Y alloys with 25.67 wt.% Y, which was positioned into the vacuum induction melting furnace. The induction furnace with a refractory lined crucible surrounded by an induction coil was located inside a vacuum chamber. The induction furnace was linked to an AC power source at a frequency precisely matched to the furnace size and then the alloy was melted under the protection of ultrahigh purity argon. The furnace was then evacuated to 1.0×10^{-2} Pa, and charged with ultrahigh purity argon. A preheated tundish-casting mold assembly was inserted through a valve. The refractory tundish was positioned in front of the induction furnace. The molten alloys were then poured through a tundish into a stainless steel cylinder with the inner diameter of 6 cm and the height of 18 cm. The mold containing hot melts was cooled down to environmental temperature under argon atmosphere in the furnace. The nominal compositions of the Mg-8Li-1Y alloy are given in Table 1 and are presented in its cast state.

Table 1 Nominal composition of the alloy (wt.%)

alloys	Mg	Li	Y
Mg-8Li-1Y	91	8	1

2.2. Electrochemical measurements

The electrochemical measurements were carried out with Princeton Applied Research in a homemade three-electrode electrochemical cell^{12,20}. The nickel foam plated by platinum was used as the auxiliary electrode. The saturated calomel electrode (SCE) was used as the reference electrode. All the potentials were quoted with respect to SCE. The working electrode was prepared as follows. The surface of the Mg-8Li-1Y alloy was successively polished with 600# and 2000# metallographic emery papers in order to make the surface smooth and remove the original oxide films on the metal surface. Then, the electrode was washed with deoxygenated ultrapure water (Milli-Q), soaked in acetone for 15 minutes to eliminate the surface grease. Finally, it was rinsed with distilled water. The dimension of the Mg-8Li-1Y electrode was 20 mm × 20 mm × 2 mm and the geometric surface area was about 0.5024 cm². The electrolyte solution was 0.7 mol L⁻¹ NaCl solution with different concentrations of Na₂SnO₃ additive. Before the experiment, the electrolyte solution was purged with N₂ gas for 10 minutes before measurements in order to remove the oxygen dissolved in the solution. During the measurements, N₂ was flowed above the solution.

Potentiodynamic polarization curves of the Mg-8Li-1Y electrode were obtained by sweeping the potential from -2.2 V to -0.8 V and the scanning rate was 5 mV s⁻¹. The corrosion current and the corrosion potential of the Mg-8Li-1Y electrode were acquired from the potentiodynamic polarization curves. Potentiostatic current-time

curves could be surveyed by keeping the Mg-8Li-1Y electrode at a scan rate of 5 mV s⁻¹ under different potentials for 15 minutes, respectively. The current density of the anodic oxidation was measured in accordance to the curves and used to analyze the oxidation activity of the electrode. Electrochemical impedance spectra were recorded under open circuit potential with the frequency range from 0.1 to 100,000 Hz and the amplitude of 5 mV.

2.3. Mg-H₂O₂ semi fuel cell tests

The performances of Mg-H₂O₂ semi-fuel cells with Mg-8Li-1Y anode were examined using a home-made flow through test cell made of stainless steel. The Mg-8Li-1Y alloy was used as the anode and the Pd coated nickel foam served as the cathode. The geometrical area of the cathode and anode was 4.0 cm² (2.0 cm × 2.0 cm). Nafion-115 membrane was used to separate the anode and the cathode compartments. The anolyte (0.7 mol L⁻¹ NaCl with 0.30 mmol L⁻¹ and without Na₂SnO₃) and the catholyte (0.7 mol L⁻¹ NaCl + 0.1 mol L⁻¹ H₂SO₄ + 0.5 mol L⁻¹ H₂O₂) were pumped into the bottom of the anode and the cathode compartments, respectively, and exited at the top of the compartments. The flow rate for the anolyte and the catholyte was 85 mL min⁻¹, which were controlled by individual peristaltic pump. The performances of the Mg-H₂O₂ were recorded using a computer-controlled E-load system (Arbin) at ambient temperature.

2.4. Characterizations of catalysts

The surface morphology of the Mg-8Li-1Y electrode was measured with scanning electron microscopy (SEM, JEOL JSM-6480). The alloy composition was determined using the energy dispersive spectrometer (EDS) with Vantage Digital Acquisition Engine (Thermo Noran, USA).

3. Results and discussion

3.1. The effect of the electrolyte additive on the potentiodynamic polarization curves of the Mg-8Li-1Y electrode

Fig. 1 shows the potentiodynamic polarization curves of the Mg-8Li-1Y electrode in 0.7 mol L⁻¹ NaCl electrolyte solution containing different concentrations of Na₂SnO₃. Table 2 displays the corrosion parameters of the Mg-8Li-1Y electrode measured in 0.7 mol L⁻¹ NaCl electrolyte solution containing different concentrations of Na₂SnO₃. The corrosion current density is significantly decreased when Na₂SnO₃ (0.05 mmol L⁻¹, 0.10 mmol L⁻¹, 0.20 mmol L⁻¹, 0.30 mmol L⁻¹) was added into the 0.7 mol L⁻¹ NaCl solution, meaning that the addition of Na₂SnO₃ to the electrolyte solution can improve the corrosion-resistive performance of the Mg-8Li-1Y electrode. The corrosion-resistive order decreases with the concentrations of Na₂SnO₃ in the following sequence: 0.20 mmol L⁻¹ (40.784 μA cm⁻²) > 0.10 mmol L⁻¹ (60.750 μA cm⁻²) > 0.05 mmol L⁻¹ (61.554 μA cm⁻²) > 0.30 mmol L⁻¹ (87.497 μA cm⁻²) > 0.00 mmol L⁻¹ (258.794 μA cm⁻²). While it is an interesting phenomenon that the corrosion current density is not monotonically dependent on the concentrations investigated. It is maybe a complicated experimental phenomenon that needs to be further studied. From our present opinion, it is maybe that the different concentrations of Na₂SnO₃ in the electrolyte solution have the different effects on the electrode surface, or have the different effects on the electrode reaction processes, which might be associated to the electrochemical impedance and the size and thickness of the micro-clumps of the products on the electrode during the reaction, thus further have a different influence on the corrosion resistance of the electrode.

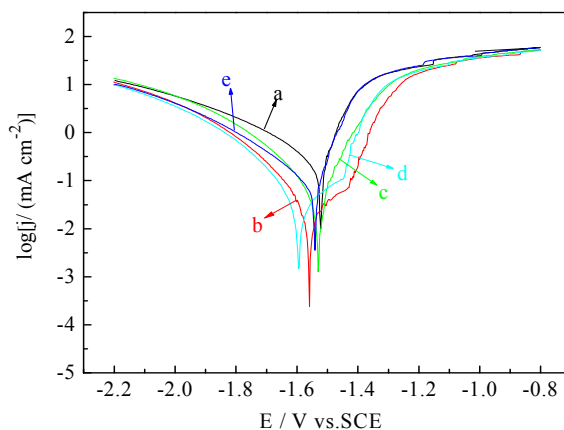


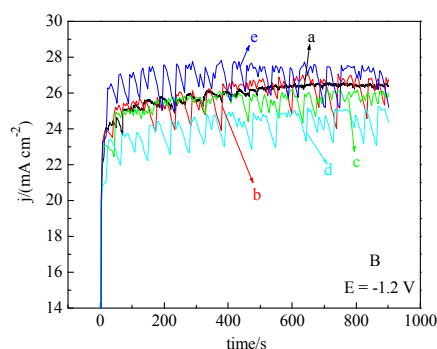
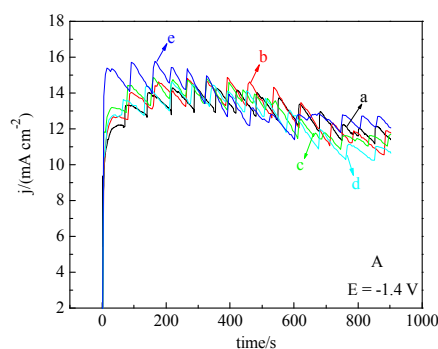
Fig. 1. The potentiodynamic polarization curves of the Mg-8Li-1Y electrode in 0.7 mol L⁻¹ NaCl solution containing different concentrations of Na₂SnO₃, (a) 0.00 mmol L⁻¹; (b) 0.05 mmol L⁻¹; (c) 0.10 mmol L⁻¹; (d) 0.20 mmol L⁻¹; (e) 0.30 mmol L⁻¹.

Table 2 The corrosion parameters of the Mg-8Li-1Y electrode measured in 0.7 mol L⁻¹ NaCl solution containing different concentrations of Na₂SnO₃ (0.00 mmol L⁻¹, 0.05 mmol L⁻¹, 0.10 mmol L⁻¹, 0.20 mmol L⁻¹ and 0.30 mmol L⁻¹).

Na ₂ SnO ₃ / mmol L ⁻¹	Corrosion potential /V (vs.SCE)	Corrosion current density/ μ A cm ⁻²	Open circuit potential/V (vs.SCE)
0	-1.522	258.794	-1.649
0.05	-1.546	61.554	-1.694
0.10	-1.534	60.750	-1.614
0.20	-1.530	40.784	-1.668
0.30	-1.552	87.497	-1.623

3.2. The effect of the electrolyte additive on the potentiostatic current-time curves of the Mg-8Li-1Y electrode

Figs. 2A, B, C and D present the potentiostatic oxidation curves of the Mg-8Li-1Y electrode at various constant potentials of -1.4 V, -1.2 V, -1.0 V and -0.8 V after the different concentrations of Na_2SnO_3 were added into 0.7 mol L^{-1} NaCl electrolyte solution, respectively. The anodic oxidation current density increases in the initial discharging stage due to the double layer charging and then decreases slightly at the corresponding discharging potentials of -1.4 V, -1.0 V and -0.8 V. Meanwhile, it can be observed from Fig. 2B that at the discharging potential of -1.2 V, the oxidation current density gradually increases with the increase in the discharging time. In addition, the larger vibrations in the current-time curves at a lower anodic potential, such as -1.4 V and -1.2 V, can be observed from Figs. 2A and B. It can be attributed to the formation and accumulation of oxidation products that prevent the Mg-8Li-1Y electrode surface from contacting with the electrolyte, leading to the decrease of active electrode surface area on the alloy surfaces. When the oxides dropped from the electrode, the electrode surface area is regenerated, and the discharging currents are bounced back.



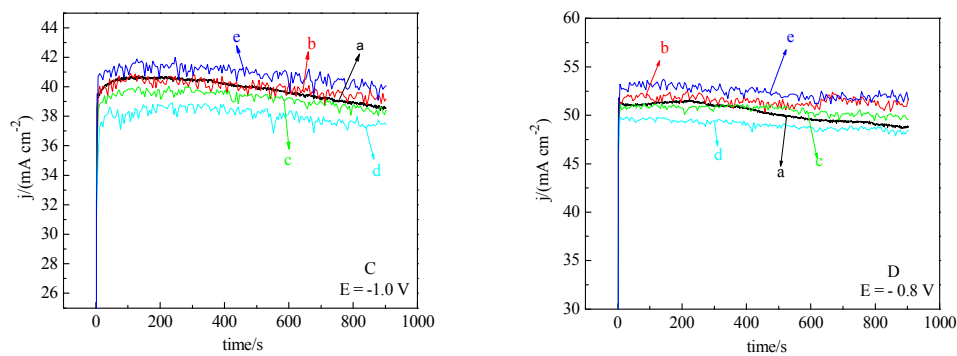


Fig. 2. The current-time curves of the Mg-8Li-1Y electrode recorded in 0.7 mol L^{-1} NaCl solution containing different concentrations of Na_2SnO_3 at various constant potentials of (A) -1.4 V , (B) -1.2 V , (C) -1.0 V and (D) -0.8 V . (a) 0.00 mmol L^{-1} ; (b) 0.05 mmol L^{-1} ; (c) 0.10 mmol L^{-1} ; (d) 0.20 mmol L^{-1} ; (e) 0.30 mmol L^{-1} .

The relatively smooth current-time profiles at anodic potentials (-1.0 V and -0.8 V) can be found in Figs. 2C and D demonstrating that the formation and shedding of oxidation products are relatively easy.

From the potentiostatic oxidation curves, it can also be observed that the discharge current density is significantly improved when $0.30 \text{ mmol L}^{-1} \text{ Na}_2\text{SnO}_3$ was added into $0.7 \text{ mol L}^{-1} \text{ NaCl}$ electrolyte solution. The stabilized discharge current density of the electrode in the presence of $0.30 \text{ mmol L}^{-1} \text{ Na}_2\text{SnO}_3$ is approximate 55 mA cm^{-2} , around 2.5 mA cm^{-2} higher than that in the absence of Na_2SnO_3 under the same discharge potential (-0.8 V). However, the Mg-8Li-1Y electrode exhibits lower discharge current density in $0.7 \text{ mol L}^{-1} \text{ NaCl}$ electrolyte solution containing $0.20 \text{ mmol L}^{-1} \text{ Na}_2\text{SnO}_3$ than that without Na_2SnO_3 under the similar experimental conditions. In the other addition concentrations of Na_2SnO_3 (0.05 mmol L^{-1} and 0.10 mmol L^{-1}), the discharge current densities of the Mg-8Li-1Y electrode exhibit no sign

of difference with no addition of Na_2SnO_3 within the test period at the tested potentials (-1.4 V, -1.2 V, -1.0 V and -0.8 V). And at the constant potential of -0.8 V, the discharge current density of the Mg-8Li-1Y electrode decreases in the following order: $0.30 \text{ mmol L}^{-1} > 0.05 \text{ mmol L}^{-1} > 0.00 \text{ mmol L}^{-1} > 0.10 \text{ mmol L}^{-1} > 0.20 \text{ mmol L}^{-1}$. As stated above, it can be concluded that the optimal addition concentration of Na_2SnO_3 is 0.30 mmol L^{-1} among the addition concentrations of Na_2SnO_3 (0.00 mmol L^{-1} , 0.05 mmol L^{-1} , 0.10 mmol L^{-1} , 0.20 mmol L^{-1} and 0.30 mmol L^{-1}).

3.3. The effect of the electrolyte additive on the impedance spectra of the Mg-8Li-1Y electrode

The impedance diagrams of the Mg-8Li-1Y electrode were measured at the open circuit potential after the different concentrations of Na_2SnO_3 were added into 0.7 mol L^{-1} NaCl electrolyte solution. The results are presented in Fig. 3. The impedance spectra recorded for the Mg-8Li-1Y electrode in all different solutions are all characterized by a single frequency capacitive semicircle. The polarization resistance R_p is represented by the diameter of the capacitive loop, as shown in Fig. 3. The polarization resistances for 0.30 mmol L^{-1} and 0.10 mmol L^{-1} addition concentrations of Na_2SnO_3 are ca. $422 \Omega \text{ cm}^{-2}$ and ca. $541 \Omega \text{ cm}^{-2}$, respectively. They are smaller than that for 0.20 mmol L^{-1} Na_2SnO_3 (ca. $618 \Omega \text{ cm}^{-2}$). The polarization resistance for 0.00 mmol L^{-1} and 0.05 mmol L^{-1} Na_2SnO_3 are similar. The polarization resistance of the Mg-8Li-1Y electrode can be arranged according to the decrease of the capacitive loop in the following order: $0.20 \text{ mmol L}^{-1} > 0.00 \text{ mmol L}^{-1} > 0.05 \text{ mmol L}^{-1} > 0.10 \text{ mmol L}^{-1} > 0.30 \text{ mmol L}^{-1}$. According to the literatures^{21,22} about impedance studies

on conventional magnesium alloys, the frequency capacitive loop acquired in the impedance spectra of the Mg-8Li-1Y electrode may result from charge transfer. This indicates that the Mg-8Li-1Y electrode with 0.30 mmol L^{-1} Na_2SnO_3 in electrolyte solution presents the most active behavior compared with the Mg-8Li-1Y electrode in the electrolyte solution with the other concentrations of Na_2SnO_3 . This result is in parallel with the results obtained from the potentiostatic current-time measurements (Figs. 2A, B, C and D).

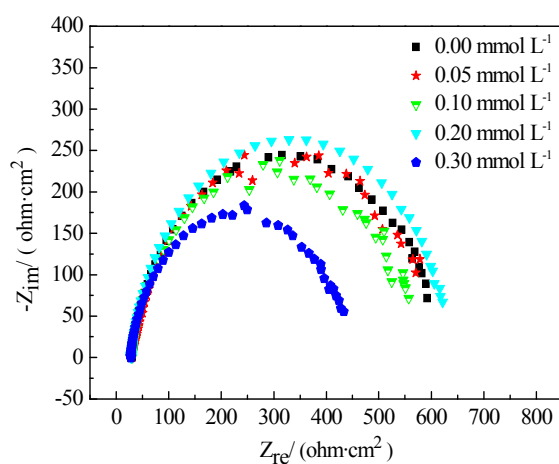


Fig. 3. The impedance spectra of the Mg-8Li-1Y electrode recorded in 0.7 mol L^{-1} NaCl solution containing different concentrations of Na_2SnO_3 .

3.4. The effects of the electrolyte additive on the morphology of the Mg-8Li-1Y electrode

Figs. 4a and b present the surface morphologies of the Mg-8Li-1Y alloys after the samples were consecutively discharged at -1.4 V , -1.2 V , -1.0 V and -0.8 V each for 15 minutes in 0.7 mol L^{-1} NaCl electrolyte solution and in 0.7 mol L^{-1} NaCl electrolyte solution containing 0.30 mmol L^{-1} Na_2SnO_3 , respectively. Clearly, the

morphologies of the oxidized surface of the Mg-8Li-1Y alloy in the absence and presence of Na_2SnO_3 are different. It was found from Fig. 4a that the oxidation products of the Mg-8Li-1Y alloy in 0.7 mol L^{-1} NaCl electrolyte solution without Na_2SnO_3 present relatively large and dense micro-blocks on the surface, which can prevent the alloy surface from contacting with the electrolyte, leading to the decrease of the active electrode surface area. Meanwhile, it can also be observed from Fig. 4b that the addition of 0.30 mmol L^{-1} Na_2SnO_3 to the electrolyte solution can markedly change the morphology of the oxidized surfaces of the Mg-8Li-1Y alloy tested. The product particles become homogeneous, loosely packed and much deep. Especially, the large channels are observed, which allows the electrolyte to penetrate through more easily. Consequently, the discharge performance of the Mg-8Li-1Y electrode is enhanced. This result is consistent with the above-mentioned observation of the potentiostatic current-time curves (Figs. 2A, B, C and D).

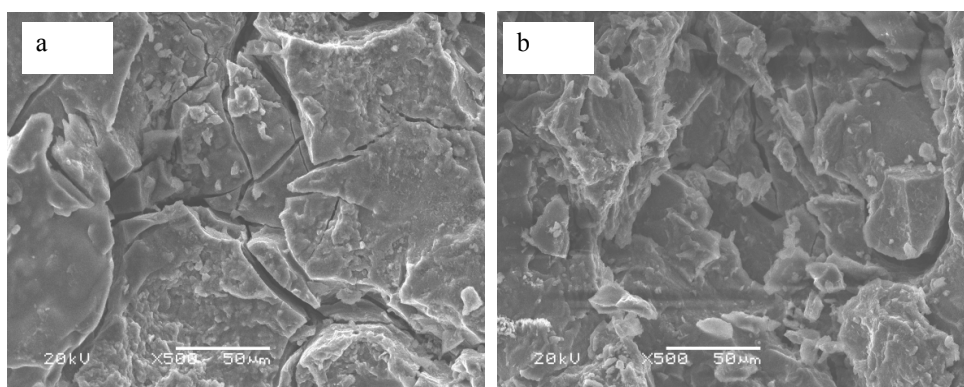


Fig. 4. The SEM micrographs of the Mg-8Li-1Y electrodes after the samples were consecutively discharged at -1.4 V , -1.2 V , -1.0 V and -0.8 V each for 15 minutes in (a) 0.7 mol L^{-1} NaCl solution and (b) 0.7 mol L^{-1} NaCl solution containing 0.30 mmol L^{-1} Na_2SnO_3 .

3.5. Fuel cell performance

In order to evaluate the effect of Na_2SnO_3 as the electrolyte additive on the performances of the Mg-8Li-1Y alloy as the anode of metal-hydrogen peroxide semi-fuel cell, the Mg- H_2O_2 semi-fuel cells were assembled and tested in 0.7 mol L^{-1} NaCl electrolyte solution and 0.7 mol L^{-1} NaCl electrolyte solution containing 0.30 mmol L^{-1} Na_2SnO_3 at ambient temperature, respectively. The experimental results are shown in Fig. 5 and Fig. 6.

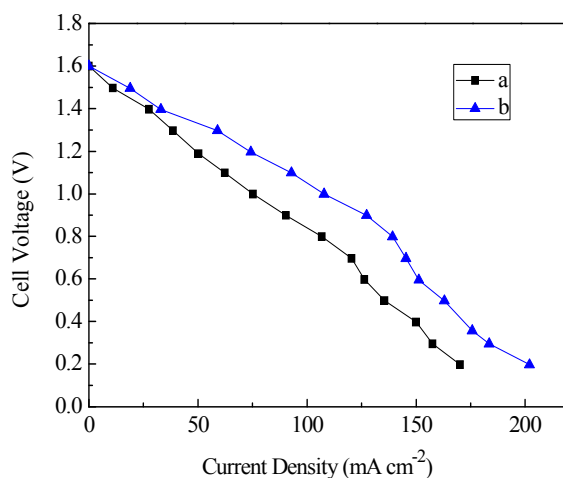


Fig. 5. The plots of the cell voltage vs. current density for Mg- H_2O_2 semi fuel cells with Mg-8Li-1Y anode in (a) 0.7 mol L^{-1} NaCl solution; (b) 0.7 mol L^{-1} NaCl + 0.30 mmol L^{-1} Na_2SnO_3 solution at room temperature. Cathode: Ir/Pd/Ni-foam. Anolyte: 0.7 mol L^{-1} NaCl. Catholyte: 0.7 mol L^{-1} NaCl + 0.5 mol L^{-1} H_2O_2 + 0.1 mol L^{-1} H_2SO_4 . Flow rate: 85 mL min^{-1} .

Fig. 5 shows the cell voltage versus current density plots. It can be seen that the gap of voltage of the cell with 0.30 mmol L^{-1} Na_2SnO_3 as the electrolyte additive and without electrolyte additive is not obvious at current density lower than 30 mA cm^{-2} . However, with the increase of current density, the presence of 0.30 mmol L^{-1} Na_2SnO_3

as the additive in the electrolyte solution can promote the cell performances distinctly. Especially at current density between 130 mA cm^{-2} and 140 mA cm^{-2} , the voltage of the cell with $0.30 \text{ mmol L}^{-1} \text{ Na}_2\text{SnO}_3$ as the additive in the electrolyte solution is around 300 mV higher than that without additive in the electrolyte solution.

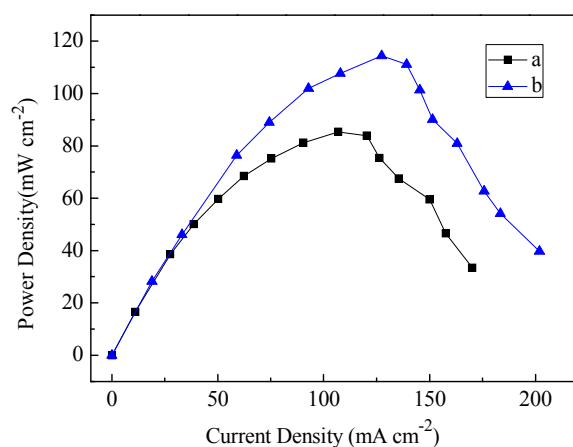


Fig. 6. The plots of the power density vs. current density for Mg- H_2O_2 semi fuel cells with Mg-8Li-1Y anode in (a) $0.7 \text{ mol L}^{-1} \text{ NaCl}$ solution; (b) $0.7 \text{ mol L}^{-1} \text{ NaCl} + 0.30 \text{ mmol L}^{-1} \text{ Na}_2\text{SnO}_3$ solution at room temperature. Cathode: Ir/Pd/Ni-foam. Anolyte: $0.7 \text{ mol L}^{-1} \text{ NaCl}$. Catholyte: $0.7 \text{ mol L}^{-1} \text{ NaCl} + 0.5 \text{ mol L}^{-1} \text{ H}_2\text{O}_2 + 0.1 \text{ mol L}^{-1} \text{ H}_2\text{SO}_4$. Flow rate: 85 mL min^{-1} .

Fig. 6 shows the curves of the power density versus current density. The peak power density of the semi-fuel cell with the Mg-8Li-1Y anode in $0.7 \text{ mol L}^{-1} \text{ NaCl}$ anolyte solution containing $0.30 \text{ mmol L}^{-1} \text{ Na}_2\text{SnO}_3$ reaches 112 mW cm^{-2} , which is higher than that containing $0.00 \text{ mmol L}^{-1} \text{ Na}_2\text{SnO}_3$ (83 mW cm^{-2}), indicating that Mg-8Li-1Y electrode as the anode of Mg- H_2O_2 semi-fuel cells with 0.30 mmol L^{-1} electrolyte additive displays better performances than that of without the electrolyte additive. And the Na_2SnO_3 as the electrolyte additive can promote the performances of

the Mg-H₂O₂ semi-fuel cells with Mg-8Li-1Y as the anode. The possible promotion mechanism will need further study.

4. Conclusions

Casting ingots of the Mg-8Li-1Y alloy as the potential anode material was prepared by the induction melting method. Its electrochemical performances in 0.7 mol L⁻¹ NaCl electrolyte solution with the different concentrations of Na₂SnO₃ were investigated. The obtained results support the following conclusions.

- (1) The corrosion current density of the Mg-8Li-1Y electrode is significantly decreased after the additive of Na₂SnO₃ is added into the electrolyte solution and thus, the corrosion resistance of the electrode is improved. Especially, the corrosion current density of the electrode reduces from 258.794 μA cm⁻² to 40.784 μA cm⁻² after 0.20 mmol L⁻¹ Na₂SnO₃ was added into 0.7 mol L⁻¹ NaCl electrolyte solution.
- (2) The discharge current density of the Mg-8Li-1Y electrode is improved by adding 0.30 mmol L⁻¹ Na₂SnO₃ to 0.7 mol L⁻¹ NaCl electrolyte solution, which is about 2.5 mA cm⁻² higher than that in 0.7 mol L⁻¹ NaCl electrolyte solution without Na₂SnO₃ under the discharge potential of -0.8 V. Na₂SnO₃ can activate and promote the discharge performances of the Mg-8Li-1Y electrode. Therefore, it is an effective electrolyte additive. The effect of the concentration of Na₂SnO₃ in electrolyte solution on the polarization resistance of the Mg-8Li-1Y electrode decreases in the following order: 0.20 mmol L⁻¹ > 0.00 mmol L⁻¹ > 0.05 mmol L⁻¹ > 0.10 mmol L⁻¹ > 0.30 mmol L⁻¹.
- (3) The addition of 0.30 mmol L⁻¹ Na₂SnO₃ into the electrolyte solution can markedly

alter the size and thickness of the micro-clumps of the oxidation products formed during discharge of the Mg-8Li-1Y electrode. Therefore, the oxidation products become small, homogeneous and deep. Then, it is convenient to allow the electrolyte to penetrate through, leading to the high discharge activity of the Mg-8Li-1Y electrode.

- (4) The voltage of the cell with $0.7 \text{ mol L}^{-1} \text{ NaCl} + 0.30 \text{ mmol L}^{-1} \text{ Na}_2\text{SnO}_3$ as the anolyte solution is around 300 mV higher than that with $0.7 \text{ mol L}^{-1} \text{ NaCl}$ as the anolyte solution at current density between 130 mA cm^{-2} and 140 mA cm^{-2} . The peak power density of the semi-fuel cell with the Mg-8Li-1Y alloy as the anode in $0.7 \text{ mol L}^{-1} \text{ NaCl}$ solution containing $0.30 \text{ mmol L}^{-1} \text{ Na}_2\text{SnO}_3$ (112 mW cm^{-2}) is higher than that in $0.7 \text{ mol L}^{-1} \text{ NaCl}$ solution (83 mW cm^{-2}).

Acknowledgements

This work was financially supported by the National Natural Science Foundation of China (21203040) and the Natural Science Foundation of Heilongjiang Province of China (B201201).

References

1. M.G. Medeiros, R.R. Bessette, C.M. Deschenes, C.J. Patrissi, L.G. Carreiro, S.P. Tucker, D. W. Atwater, *J. Power Sources*, 2004, 136, 226-231.
2. O. Hasvold, N. J. Storkersen, S. Forseth, T. Lian, *J. Power Sources*, 2006, 162, 935-942.
3. D. J. Brodrecht, J. J. Rusek, *Appl. Energ.* 2003, 74, 113-124.
4. W. Yang, S. Yang, W. Sun, G. Sun, Q. Xin, *J. Power Sources* 2006, 160,1420-1424.
5. W. Yang, S. Yang, W. Sun, G. Sun, Q. Xin, *Electrochim. Acta*, 2006, 52, 9-14.

6. R. R. Bessette, J. M. Cichon, D. W. Dischert, E. G. Dow, *J. Power Sources*, 1999, 80, 248-253.
7. R. R. Bessette, M. G. Medeiros, C. J. Patrissi, C. M. Deschenes, C. N. LaFratta, *J. Power Sources*, 2001, 96, 240-244.
8. M. G. Medeiros, C. G. Zoski, *J. Phy. Chem. B*. 1998, 102, 9908-9914.
9. R. P. Hamlen, D. W. Atwater, in: D. Linden, T.B. Reddy (Eds.), *Handbook of Batteries, third ed.*, McGraw-Hill, 2002, p. 381.
10. E. G. Dow, R. R. Bessette, M. G. Medeiros, H. Meunier, G. L. Seebach, J. Van Zee, C. Marsh-Orndorff, *J. Power Sources*, 1997, 65, 207-212.
11. C. Marsh, H. Munier, R. Bessette, M. G. Medeiros, J. Van Zee, G. Seebach, An effective method for the reduction of H₂O₂, US Patent #5, 296, 429.
12. D. X. Cao, L. Wu, Y. Sun, G. L. Wang, Y. Z. Lv, *J. Power Sources*, 2008, 177 624-630.
13. Y. Z. Lv, Y. Xu, D. X. Cao, *J. Power Sources*, 2011, 196, 8809-8814.
14. Y. Z. Lv, M. Liu, D. X. Cao, *J. Power Sources*, 2013, 225, 124-128.
15. Y. Z. Lv, M. Liu, Y. Xu, D. X. Cao, J. Feng, R. Z. Wu, M. L. Zhang, *J. Power Sources*, 2013, 239, 265-268.
16. I. J. Albert, M. A. Kulandainathan, M. Ganesan, V. Kapali, *J. Appl. Electrochem.* 1989,19,547-551.
17. M. L. Doche, F. Novel-Cattin, R. Durand, J. J. Rameau, *J. Power Sources*, 1997, 65, 197-205.
18. V. Kapali, S. V. Iyer, V. Balaramachandran, K. B. Sarangapani, M. Ganesan, M. A. Kulandainathan, A. Sheik Mideen, *J. Power Sources* 1992, 39, 263-269.
19. K. B. Sarangapani, V. Balaramachandran, V. Kapali, S. V. Iyer, M. G. Potdar, K. S. Rajagopalan, *J. Appl. Electrochem.* 1984, 14, 475-480.

20. D. X. Cao, L. Wu, G. L. Wang, Y. Z. Lv, *J. Power Sources*, 2008, 183, 799-804.
21. Anik M., Celikten G., *J. Corrosion Science*, 2007, 49, 1878-1894.
22. Song G, Atrens A, Wu X. et al., *J. Corrosion Science*, 1998, 40, 1769-1791.